DYNAMICS OF THE GAS-PLASMA TORCH FORMED BY THE HIGH-CURRENT ELECTRON BEAM ACTION ON SOLID TARGETS

V.F. Klepikov, V.V. Lytvynenko*, Yu.F. Lonin, A.G. Ponomarev, O.G. Tolstolutskiy, V.V. Uvarov, V.T.Uvarov*

NSC "Kharkov Institute of Physics and Technology", Kharkov, Ukraine;
**Institute of Electrophysics and Radiation Technologies of NASU, Kharkov, Ukraine*

The interaction of high-current REB with the surface of solid targets was investigated. The target material was stainless steel 12X18H10T, graphite, tungsten, plexiglas. The optical diagnostic methods were used to determine the space-time characteristics of a gas-plasma torch (GPT), formed as a result of the tubular microsecond REB action on the surface of solid targets. The times of GPT formation and its spread velocity (transverse and longitudinal) for different materials were determined. An axial focus of GPT, moving towards the beam, was found.
PACS: 79.20.Kz

INTRODUCTION

Interaction between the concentrated energy fluxes and the material is accompanied by many physical phenomena: material heating and evaporation, gas-plasma torch (GPT) [1] formation and expansion, vapor condensation, chemical transformations, phase composition change, radiation defect formation, shock wave arising, high pressure appearance etc [2,3]. This wide range of phenomena is extending due to the factors influencing on the energy transport to the target material.

Application of diagnostic optical methods at the accelerator MIG-1 [4] has provided the most complete information about the GPT spread dynamics under action of tubular REB on the solid targets. The research data can be useful for investigations on the interaction of concentrated plasma flows and charged particles with first-wall materials and divertor plates.

1. RESEARCH TECHNIQUE AND EXPERIMENTAL PROCEDURE

To investigate the space-time characteristics of GPT we used the field density visualization method on the base of geometrical deviations of parallel light beams on optical inhomogeneities – schlieren method [5] and the method of high-speed/fast photographing.

Fig.1 presents the diagram of the experiment on the optical diagnostics of the gas-plasma torch obtained by these methods. In the experiment both the disk target and the combined target were irradiated with the tubular high-current REB having the following parameters: energy ~ 0.5 MeV, current ~ to 4 kA, current pulse duration of (2… 5)·10^{-6} s. The followings samples were investigated: stainless steel 12X18H10T, graphite, tungsten, plexiglas.

The velocities of GPT and target material liquid phase spread in the longitudinal and transverse directions were determined from the shadow photographs by measuring the opacity zone boundary displacement for a laser probe radiation with a wave length of 0.53 μm and an exposure time of 20 s. The radiation of a laser LTI-PCH was transformed by the optical system (telescopes with a focal distance of 750 mm), so that the space before the target be illuminated by the parallel luminous flux, and the interaction space image be projected onto the recording element (photographic film).

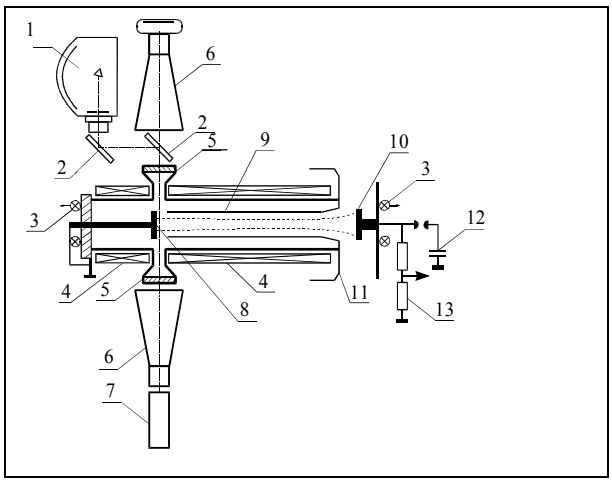

Fig.1. Scheme of optical diagnostics: 1 – SPhR-2M; 2 – mirror; 3 – Rogowski loop; 4 – solenoid; 5 – window; 6 – telescope; 7 – laser LTI-PCH -5; 8 – target-collector; 9 – tubular insertion; 10 – cathode; 11 – anode; 12 – high-voltage generator; 13 – voltage divider

The delay time of light radiation generation in relation to the time of REB-target interaction beginning was varying to obtain the pictures of zones, opaque to a light probe radiation in different instants of time.

The space-time characteristics of GPT, formed as a result of the high-current REB action onto the solid targets were also measured by means of a high-speed photorecorder SPhR-2M, working in the mode of continuous scan.

The optical radiation output from the interaction volume has been carried out through the slits of 1.5 cm width and 8.0 cm height, located on the opposite sides of a vacuum chamber. The magnetic field is weighted down in the area of slits was insignificant (to 10 %), that practically has no influence on the quality of the transported high-current REB [6].

Thus, the electron beam was reliably closed on the grounded anode without distortions of current

characteristics. And the character of the tubular high-current REB interaction with combined targets and disk targets was almost unchangeable.

2. EXPERIMENTAL RESULTS

2.1. GPT SPREAD FROM GRAPHITE

The shadowgraphs of the tubular high-current REB interaction with graphite targets, made in the form of disk, and as a combined target, are shown in Fig.2a. It is seen that GPT forming and its spread begins only $5 \cdot 10^{-6}$ s after the collector current pulse start (beam arrival on the target) and continues during long time > $1.5 \cdot 10^{-5}$ s after the pulse ceasing. The measured longitudinal velocity of GPT spread from the graphite target was (0.44… 1.0)$\cdot 10^5$ cm/s, and the transverse velocity was measured by shadowgraphs on the combined target (Fig.2b) as it can not be estimated on the disk target because its central area is shaded for observation by the ring GPT. The graphite strip of 5 mm width was fastened at a distance of 50 mm from the disk

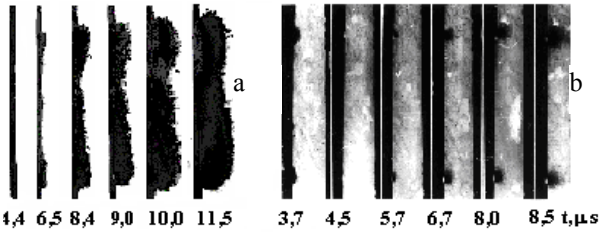

Fig.2. Flying away of GPT from a graphite target: a – disk; b – strip

In the point of REB impact on the graphite strip-target (Fig.2b), 3.7 μs after, one can observe a brightly glowing heat-penetration zone having a depth of 0.7 mm and a width of 1.8 mm (the width of the tubular beam ring is 1.0 mm).

2.2. GPT SPREAD FROM STEEL 12X18H10T

Shadowgraphs obtained for the tubular REB interaction with a target made from steel 12X18H10T (Fig. 3) differ sharply from the shadowgraphs obtained on graphite. There is no a brightly glowing heat-penetration zone in the point of beam impact on the stainless steel, and the GPT formation and spread occurs much more earlier than in $2 \cdot 10^{-6}$ s after the REB current pulse start and continues more than $3.5 \cdot 10^{-5}$ s.

Fig.3. GPT spread from steel 12X18H10T (strip target)

As is seen from the shadow photographs in Fig. 3, the measured spread velocities of GPT made of 12X18H10T steel are several times higher than the spread velocities of GPT from graphite. So, the longitudinal spread velocity of GPT from steel 12X18H10T is in the range (0.8… 4.0)$\cdot 10^5$ cm/s, and the transverse one is in the range (1.25…2.15)$\cdot 10^5$ cm/s.

However, the main difference in the shadowgraphs, obtained on irradiated steel 12X18H10T under irradiation, consists in the following: 8 μs after the current pulse start in the central axial zone, where the beam has no effect on the target, a zone arises being first narrow and subsequently expanding (GPT axial focus) and, also, opaque to the laser probe radiation($\lambda = 0.53$ μm), which exists during long time ~ $2 \cdot 10^{-5}$ s.

The shadowgraphs in Fig. 4 represent the front part of GPT from the target of steel 12X18H10T (in the form of a strip) and the rear part of the central axial GPT. It is seen, that the central axial GPT, at the beginning of GPT is a very heated gas of a high density and partially ionized with atoms of target material. As a result, the GPT spread occurs with high velocities, and due to the recoil momentum a powerful cylindrical shock wave arises. The shock wave front propagates from the REB impact point on the target with velocities of (0.5…4)$\cdot 10^5$ cm/s.

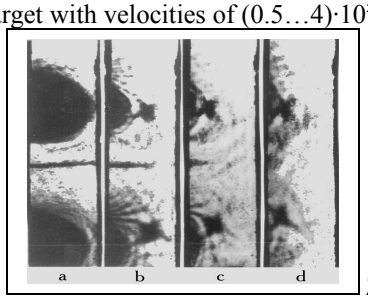

Fig.4. Leading edge of flying away of GPT from steel of 12X18H10T time of delay of $t_з$ = 8.5 μs: a- 5 mm, b -10 mm, c-15 mm, d -16.5 mm

The measured velocities of longitudinal and lateral expansion of this axial zone were (5…7)$\cdot 10^5$ cm/s and (1…2)$\cdot 10^5$ cm/s respectively.

Similar shadowgraphs with an opaque zone in the near-axial area of the beam at the target surface were also obtained for the interaction between the tubular REB and the tungsten targets and plexiglas targets.

2.3. SCANNING PHOTOGRAPHIC RECORDS OF THE GLOW FROM STEEL 12X18H10T

The dynamics of GPT forming and spreading was determined from the scanning photographic records (SPhR) obtained during the tubular REB action on the disk targets and combined targets of (1…10) mm thickness.

Photographic scans obtained at different distances of the recorder limiting slit from the strip-target made from steel 12X18H10T are shown in Fig.5.

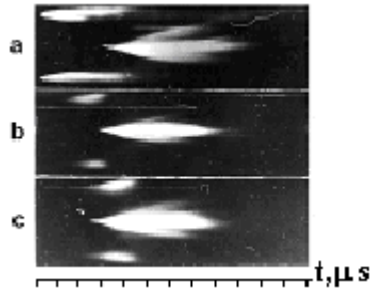

Fig.5. Photographic scans of GPT glowing from steel 12X18H10T at different distances of the recorder slit from the strip- target surface: a) z=0 mm, b) z = 7.5 mm, c) z = 15 mm (1 div = 2 μs)

The GPT glow arises at the target surface in the point of tubular REB action. After $7 \cdot 10^{-6}$ s (for steel 12X18H10T), i.e. simultaneously with formation of a

zone, opaque to the laser probing radiation ($\lambda = 0.53$ μm), in the central axial part, that is seen in the shadow photographic scans, a bright glow is recorded which is continues during about $2 \cdot 10^{-5}$ s and expands in the transverse direction with a velocity of $1.2 \cdot 10^5$ m/s.

Displacement of the limiting slit of the photorecorder SPhR-2M to different distances from the target surface has shown that at the beginning of forming (in the moment of time $7 \cdot 10^{-6}$ s) the glow area of the central axial GPT has a diameter equal to ~ 10 mm, and it is limited to 25 mm. in the longitudinal direction. The diameter of the tubular REB is equal to 30 mm.

3. CONCLUSIONS

The diagnostic optical methods were applied to investigate the processes of microsecond REB interaction with the surface of solid targets. The longitudinal and transverse velocities of GPT spread are determined. It is shown that the velocities of GPT spread from steel 12X18H10T are several times higher than the GPT spread velocities for graphite, the REB parameters being unchangeable.

The mechanism of GPT generation and expansion under action of a tubular high-current REB (the power density equals to ~ $10^8 \ldots 10^{10}$ W/cm^2) on the surface of solid targets is involved by the irradiated surface ablation due to its superheating, melting and evaporation and by the formation of powerful cylindrical shock waves, the fronts of which are converging on the drift chamber axis and form a gas-plasma focus.

The glow, recorded in SPR records, is a very heated gas and plasma with excited and partially ionized atoms of the target material. The GPT focus also is a heated gas-plasma but with higher values of density and temperature, as compared to the near-target GPT. A maximum of the GPT focus beginning from 8 μs after its formation and during all the time of existence (to $1.5 \cdot 10^{-5}$ s) does not change its position and is at a distance of (2…3) mm from the surface of the target (12X18H10T) under irradiation up to the spread start with a velocity of ~ $4 \cdot 10^5$ cm/s. The brightest glow arises on the drift chamber axis where the beam in the form of cylinder is absent.

It has been established that the GPT spread from steel 12X18H10T begins ~ 2 μs after the current pulse start. Just this time determines the lifetime of the metastable state as an ablation precursor.

REFERENCES

1. J. Dudertstadt, G. Moses. *Inertial nuclear fusion*. M.: "Energoatomizdat", 1984, p.141–142 (in Russian).
2. Ya.B. Zeldovich, Yu.R. Rayzer. *Physics of shock waves and high-temperature hydrodynamic phenomena.* M.: "Nauka", 1966 (in Russian).
3. B.A. Demidov, A.I. Martynov. Experimental investigation of shock waves excited by high-current relativistic electron beam in metals // *Zhurnal Ehksperimental'noj i Tekhnicheskoj Fiziki.* 1981, N2, p.729–744 (in Russian).
4. V.T. Uvarov, Yu.V. Tkach, N.P. Gadetsky et al. *Production of microsecond high-current beams of a high efficiency:* Preprint. Kharkov: Institute of Physics and Technology, M.: "TsNII AtomInform", 1984 (in Russian).
5. D. Holder, D. Nort. *Shadow methods in aerodynamics*. M.: "Mir", 1966 (in Russian).
6. A.M. Egorov, V.F. Klepikov, A.G. Ponomaryov, A.G. Tolstolutsky, V.V. Uvarov, V.T. Uvarov. Optical diagnostics of the collector plasma // *Visnyk Kharkivs'kogo Natsionalnogo Universitetu. Series: Physics:"Nuclei, particle, fields".* 2001, N 510, Part 1(13), p.62–67 (in Ukrainian).

Article received 2.10.08

ДИНАМИКА ГАЗОПЛАЗМЕННОГО ФАКЕЛА ПРИ ВОЗДЕЙСТВИИ СИЛЬНОТОЧНЫХ РЭП НА ТВЕРДОТЕЛЬНЫЕ МИШЕНИ

В.Ф. Клепиков, В.В. Литвиненко, Ю.Ф. Лонин, А.Г. Пономарев, А.Г. Толстолуцкий, В.В. Уваров, В.Т. Уваров

Исследовалось взаимодействие сильноточного РЭП с поверхностью твердотельных мишеней, в качестве которых служили нержавеющая сталь 12Х18Н10Т, графит, вольфрам, оргстекло. С помощью оптических методов диагностики получены пространственно-временные характеристики газоплазменного факела (ГПФ), образованного при воздействии трубчатых релятивистских электронных пучков микросекундной длительности на поверхность твердотельных мишеней. Определены времена образования ГПФ, поперечная и продольная скорости его разлета для различных материалов. Обнаружено образование осевого фокуса ГПФ, который распространяется навстречу пучку.

ДИНАМІКА ГАЗОПЛАЗМОВОГО ФАКЕЛА ПРИ ВПЛИВІ СИЛЬНОСТРУМОВИХ РЕП НА ТВЕРДОТІЛЬНІ МІШЕНІ

В.Ф. Клепіков, В.В. Литвиненко, Ю.Ф. Лонін, А.Г. Пономарьов, О.Г. Толстолуцький, В.В. Уваров, В.Т. Уваров

Досліджувалась взаємодія сильнострумового РЕП з поверхнею твердотільних мішеней, в якості котрих були нержавіюча сталь 12Х18Н10Т, графіт, вольфрам та органічне скло. За допомогою оптичних методів діагностики отримано просторово-часові характеристики газоплазмового факела (ГПФ), який утворювався при дії трубчастих РЕП мікросекундної тривалості на поверхню твердотільних мішеней. Отримано час утворення газоплазмового факела, поперечна і повздовжня швидкість його розльоту для різних матеріалів. Виявлено утворення осьового фокуса ГПФ, який рухається назустріч пучку.